CU Journal of Non-Linear Fluid Mechanics
Vol. 01, No. 01, 2025
https://doi.org/10.11615/cujnlfm.01104-5

Heat and mass transfer effect on chemically reactive bi-viscous Bingham hybrid nanofluid flow over permeable surface with inclined magnetic field

S. M. Sachhin[a], U. S. Mahabaleshwar *[a], S. N. Ravichandra Nayakar[b], O. Manca[c] & Mikhail A. Sheremet[d]

[a] Department of Studies in Mathematics, Davangere University, Shivagangothri, Davangere, 577007, India.
[b] Department of Mathematics, University BDT College of Engineering, Davangere, India.
[c] Dipartimento di Ingegneria, Universitàdegli Studidella Campania Luigi Vanvitelli, Aversa, CE, Italy.
[d] Laboratory on Convective Heat and Mass Transfer, Tomsk State University, 634050 Tomsk, Russia.

Abstract
The current work aims to analyze the impact of Brinkman number and variable MHD on Bi-viscous Bingham hybrid nanofluid flow across the penetrable sheet with heat transfer. Molybdenum disulfide (MoS_2) and Graphite oxide (GO) nanoparticles are dispersed in Sodium alginate (*SA*) to form a hybrid nanofluid. Using similarity conversions, the governing nonlinear PDEs for momentum, temperature, and concentration are transformed into ODEs along with the boundary condition. In the fluid region, the heat balance is kept conservative with a source/sink that relies on the temperature, and in the case of radiation, Bvp-4c, and shooting method to obtain the numerical solutions. Furthermore, the results of the current problem can be discussed by implementing a graphical representation with different factors, The results of the present analysis define that upsurging the inverse Darcy number decays the axial velocity, and increasing the thermal radiation raises the temperature. The current problem contains many industrial uses in technology and industrial processes, like Aerodynamics in vehicle design, blood flow in medicine, and oil and gas extraction.

Keywords: Thermal radiation; Heat source/sink; Inclined magnetic field; Bi-viscous Bingham fluid; Porous media.

Nomenclature

List of symbols	Descriptions	SI unit
a	Stretching coefficient	$[s^{-1}]$
A_1, A_2, A_3, A_4, A_5	Constants	[-]
C_p	Specific heat co-efficient	$[JK^{-1}Kg^{-1}]$
$f(\eta)$	Velocity function	[-]

* ✉ u.s.m@davangereuniversity.ac.in

N_r	Radiation $\left(=\frac{16\sigma^* T_\infty^3}{3k^*\kappa_f}\right)$	[-]
Pr	Prandtl term	[-]
q_r	Radiative heat flux $\left(=-\frac{4\sigma^*}{3k^*}\frac{\partial T^4}{\partial y}\right)$	$[Wm^{-2}]$
T_w	Surface Temperature	$[K]$
T	Temperature	$[K]$
T_∞	Ambient temperature	$[K]$
u, v	x, y axis momentum fluid phase	$[ms^{-1}]$
u_w	Velocity	$[ms^{-1}]$
v_w	Wall velocity	$[ms^{-1}]$
x, y	Coordinates	$[m]$

Greek symbols

η	Similarity variable	[-]
κ^*	Absorption coefficient	$[m^{-1}]$
ψ	Stream function	[-]
σ^*	Stephen Boltzmann constant	$[Wm^{-2}K^{-4}]$
$\theta(\eta)$	Dimensionless Temperature	[-]
μ	Dynamic viscosity	$[kgm^{-1}s^{-1}]$
ρ	Fluid density	$[kg/m^3]$
σ	Electrical conductivity	$[S/m]$
κ	Thermal conductivity	$[kgms^{-3}K^{-1}]$
ν	Kinematic viscosity	$[m^2s^{-1}]$
η	Similarity variable	[-]

1 Introduction

Bingham fluids, characterized by their yield-stress behavior, have a wide range of applications across various industries. These viscoplastic materials behave like a solid until a certain stress threshold is exceeded, beyond which they flow like a viscous fluid. This unique property is utilized in the petroleum industry for drilling muds, which must remain stationary to support the wellbore walls but flow under applied stress to carry drill cuttings to the surface. In the food industry, products like mayonnaise and ketchup exhibit Bingham plastic behavior, allowing them to be easily spread or squeezed from containers but hold shape when at rest. The construction industry benefits from this fluid characteristic in cement and concrete handling, ensuring that these materials are workable when needed but set without sagging or spreading. Additionally, Bingham fluids play a crucial role in biomedical applications, particularly in the formulation of creams and ointments that require ease of application but also need to stay in place on the skin. The understanding and modeling of Bingham fluid flow are essential for optimizing these applications, ensuring efficient and effective use of materials with such complex rheological properties. Sachhin [1] studied the drag coefficient and magnetic effect on nanofluids by using the hypergeometric method. Wu [2] studied the moving of Bingham fluid in porous media by developing single-phase flow with integral methods. Turan [3] studied the Bingham model by using the 2-D laminar flow of nanofluid over heated side walls. Vola [4] studied the Galerkin method with convection decomposition of the movement of Bingham fluids by using constitutive law. Mahabaleshwar [5] studied the fluid flow over stretching sheets.

The Brinkman number is a dimensionless term which is relevant in the context of polymer processing and other engineering applications where heat conduction and viscous dissipation are significant factors. This parameter is instrumental in designing systems where precise temperature control is essential, such as in screw extruders used in polymer processing. In these systems, the balance between the energy supplied by the motor and the heaters is critical for the quality of the final product. Understanding and applying the Brinkman number can lead to more efficient and effective thermal management in various fluid flow scenarios. Sachhin [6] and Siddeshwar [7] explored the influence of heat transfer on nanofluid flows of Couplestress fluids with Darcy-Brinkman effects. Rahman [8] focused on a steady flow of dusty fluids flow over slip geometry with the effects of dissipation and Brinkman ratio. Zhang [9] studied the electromagnetic effect of Newtonian fluid flow with the Brinkman model. Abo [10] studied the influence of the Darcy-Brinkman model on dielectric fluid movement via the wavy sinusoidal channel. Yao [11] studied the Darcy and Brinkman equations on the fluid flow over porous media.

The interplay between chemical reactions and fluid flow is a cornerstone of numerous industrial and natural processes. In the realm of environmental engineering, this interaction is crucial for the design of efficient waste-water treatment systems, where chemical reactions are used to break down pollutants. In the field of energy, the principles of fluid dynamics and chemical kinetics are applied to optimize combustion in engines and turbines, ensuring complete fuel utilization and reduced emissions. Jena [12] studied the chemical reaction effect on Jeffrey's fluid movement of porous media and mass transfer. Damseh [13] explored the micropolar fluid movement with natural convection numerically by using the influence of chemical reactions. Patil [14] studied the influence of chemically reactive polar fluid flow via a steady plate. Khan [15] studied the effect of magnetic fluid flow over the sheet with a chemical reaction. Hosseinzadeh [16] studied the flow of chemically reactive hybrid nanofluid using Joule heating and the Darcy-Forchheimer model.

Porous media play a crucial play in the mechanics of fluid movement, impacting a wide range of usages from environmental engineering to petroleum extraction. Advances in this field continue to enhance our ability to manage natural resources and develop sustainable industrial practices. For a deeper dive into the basic theory of fluid flow in porous media, one might explore scientific literature that discusses Darcy's law and its applications in various fields. Alazmi [17] studied the interfacial expression of the porous medium and fluid surface by using different boundary conditions. Misra [18] studied the magnetic movement of blood in a capillary over the porous wall with time-dependent momentum. Elgazery [19] focused on the impact of heat generation and Darcy model on Casson nanofluid flow across the axisymmetric surface. Coulaud [20] explored the numerical solution for Navier-Stokes equations of fluid flow with the primary effects in a porous medium. Kaothekar [21] studied the ionized thermal plasma with thermal instability and astrophysical condensation via porous media.

Solar radiation plays a major role in the dynamics of fluid flow, particularly in processes where heat transfer is a significant factor. For instance, in the field of aerospace engineering, thermal radiation is a key consideration in the design of spacecraft, as it affects the thermal control systems that manage the temperatures within and on the surface of the spacecraft. In environmental engineering. These examples highlight the diverse applications of solar radiation in influencing fluid flow across various scientific and engineering disciplines. Siddeshwar [22] explored the effect of radiation on fluid movement via a sheet with slip velocity. Yu [23] focused on the movement of Carbon fluid with thermal boundary conditions. Li [24] studied the convective movement of magnetic fluid via an inner cylinder with heat transfer and velocity boundary conditions. [25, 26] studied the movement of a homogeneous second-grade liquid with solar radiation effects. [27-31] studied the effect of radiation and MHD on fluid movement over vertical plates. [32-40] explored the numerical solution for Navier-Stokes equations of fluid flow with the primary effects in a porous medium using different boundary conditions.

2 Mathematical formulations with solutions

Consider an inclined MHD and heat radiation with porous media in a biviscosity Bingham chemically reactive fluid flow across a expanding sheet. Considering the flow as laminar and incompressible, assuming a stretching velocity as $U_w = ax$ where $a > 0$. The biviscosity Bingham fluid's rheological expression as follows [1, 2]

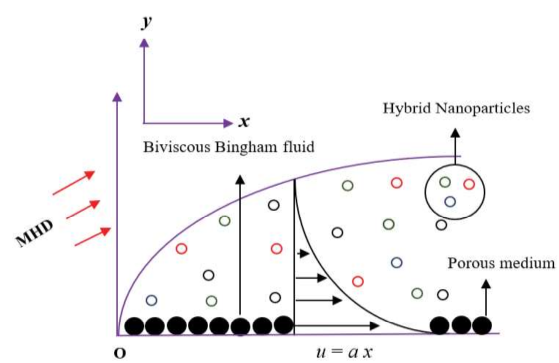

Figure 1: Schematic diagram of fluid flow.

$$\tau_{ij} = \begin{cases} 2(\mu_B + p_y / \sqrt{2\pi})e_{ij}, & \pi > \pi_c, \\ 2(\mu_B + p_y / \sqrt{2\pi_c})e_{ij}, & \pi < \pi_c, \end{cases} \quad (1)$$

where π, π_c, P_y & μ_B are deformation rate product, product value, yields stress and viscosity of plastic deformation.

The current problem's governing equations [6, 22, 28].

$$\frac{\partial u}{\partial x} + \frac{\partial v}{\partial y} = 0, \quad (2)$$

$$u\frac{\partial u}{\partial x} + v\frac{\partial u}{\partial y} = \frac{\mu_{eff}}{\rho_{hnf}}\left(1+\frac{1}{\lambda}\right)\frac{\partial^2 u}{\partial y^2} - \frac{\sigma_{hnf}}{\rho_{hnf}}B_0 \operatorname{Sin}^2(\tau)u - \left(1+\frac{1}{\lambda}\right)\frac{\nu_{hnf}}{K^*}u, \quad (3)$$

$$u\frac{\partial T}{\partial x} + v\frac{\partial T}{\partial y} = \frac{\kappa_{hnf}}{(\rho C_p)_{hnf}}\frac{\partial^2 T}{\partial y^2} - \frac{1}{(\rho C_p)_{hnf}}\frac{\partial q_r}{\partial y} + \frac{Q_0(T-T_\infty)}{(\rho C_p)_{hnf}}, \quad (4)$$

$$u\frac{\partial C}{\partial x} + v\frac{\partial C}{\partial y} = D_{hnf}\frac{\partial^2 C}{\partial y^2} - Cr^2\left(C - C_\infty\right), \quad (5)$$

B. Cs are given by [6, 22, 28].

$$u = ax, \quad v = 0 \quad T = T_w, \quad C = C_w \quad \text{as} \quad y \to 0,$$

$$u = 0, \quad T = T_\infty, \quad C = C_\infty \quad \text{at} \quad y \to \infty, \quad (6)$$

where u and v are momentum terms. λ, ν, $B_0 \operatorname{Sin}^2 \tau$, ρ, κ, σ are the biviscosity Bingham fluid parameter, viscosity, inclined MHD, density, thermal conductivity, electrical conductivity,

Similarity transformations are given as [18, 22, 28]:

$$u = axf_\eta(\eta), \quad v = -\sqrt{a\nu}\, f(\eta), \quad \eta = y\sqrt{\frac{a}{\nu}}, \quad \theta(\eta) = \frac{T - T_\infty}{T_w - T_\infty}, \quad \varphi(\eta) = \frac{C - C_\infty}{C_w - C_\infty} \quad (7)$$

By using Rosseland's approach radiation heat flux q_r is formulated [6, 18, 28] as:

$$q_r = -\frac{4\sigma^*}{3\,k^*}\frac{\partial T^4}{\partial y}, \quad (8)$$

$$T^4 \cong 4T_\infty^3 T - 3T_\infty^4. \quad (9)$$

The radiation term in Eq. (4) is calculated as:

$$\frac{\partial q_r}{\partial y} = -\frac{16\,\sigma^* {T_\infty}^3}{3\,k^*}\frac{\partial^2 T}{\partial y^2}. \tag{10}$$

Combining equations (10) and (4) we get:

$$u\,\frac{\partial T}{\partial x} + v\,\frac{\partial T}{\partial y} = \left(\frac{\kappa}{(\rho C_p)_{hnf}} - \frac{1}{(\rho C_p)_{hnf}}\frac{16\,\sigma^* {T_\infty}^3}{3\,k^*}\right)\frac{\partial^2 T}{\partial y^2} + \frac{Q_0(T-T_\infty)}{(\rho C_p)_{hnf}}, \tag{11}$$

by using similarity transformations, equations (3) and (4) simplifies to:

$$\left(1+\frac{1}{\lambda}\right)\Lambda f_{\eta\eta\eta}(\eta) - \frac{A_2}{A_1}\left[f_\eta(\eta)\right]^2 + \frac{A_2}{A_1}f_{\eta\eta}(\eta)f(\eta) - \left\{\frac{A_3}{A_1}MS\text{in}^2(\tau) + \left(1+\frac{1}{\lambda}\right)Da^{-1}\right\}f_\eta(\eta) = 0, \tag{12}$$

$$(A_4 + N_r)\theta_{\eta\eta}(\eta) + A_5 \Pr\theta_\eta(\eta)f(\eta) + N_i \Pr\theta(\eta) = 0\,, \tag{13}$$

$$A_6\varphi_{\eta\eta}(\eta) + Sc\,f(\eta)\varphi_\eta(\eta) - Sc\,Cr^*\varphi(\eta) = 0. \tag{14}$$

where

$M = \dfrac{\sigma_f B_0^2}{\rho_f a}$, is the magnetic field term,

$Cr^* = \dfrac{Cr^2}{a}$, Chemical reaction parameter,

$Da^{-1} = \dfrac{\nu_f}{K^* a}$, is the inverse Darcy number,

$N_i = \dfrac{Q_0}{(\rho C_p)_f}$, is the Heat source/sink,

$Sc = \dfrac{\nu_f}{D_f}$, are Schmidt number,

$$A_1 = \frac{\mu_{hnf}}{\mu_f},\ A_2 = \frac{\rho_{hnf}}{\rho_f},\ A_3 = \frac{\sigma_{hnf}}{\sigma_f},\ A_4 = \frac{\kappa_{hnf}}{\kappa_f},\ A_5 = \frac{(\rho C_p)_{hnf}}{(\rho C_p)_f},\ A_6 = \frac{D_{hnf}}{D_f}.$$

The modified boundary conditions are as follows [1, 6, 22, 28]:

$$f(\eta)=0,\quad f_\eta(\eta)=1,\quad \theta(\eta)=1,\quad \varphi(\eta)=1 \quad \text{as} \quad \eta\to 0,$$

$$f_\eta(\eta)=0,\quad \theta(\eta)=0,\quad f_{\eta\eta}(\eta)=0,\quad \varphi(\eta)=0, \quad \text{at} \quad \eta\to\infty$$

. (15)

Nusselt number is calculated as:

$$Nu = \frac{xq_w}{\kappa_{hnf}(T_w - T_\infty)} \quad ,$$

where

$$q_w = -\left(\left(\frac{16\sigma^* T_\infty^3}{3k^*} + \kappa_{hnf}\right)\right)\left(\frac{\partial T}{\partial y}\right)_{y=0}$$ is the heat flux at the wall.

Skin Friction Calculation [6, 18, 22]:

Skin frictions calculated as

$$C_f = \frac{\tau_w}{\rho_f} = \left(1 + \frac{1}{\lambda}\right)\frac{\mu_{eff}}{\rho_f U_w^{\ 2}} \left.\frac{\partial u}{\partial y}\right|_{y=o} ,$$

The skin friction is calculated as

$\mathrm{Re}^{1/2} C_f = \Lambda \left(1 + \frac{1}{\lambda}\right) f_{\eta\eta}(0),$

Where

$$Nu\mathrm{Re}^{-1/2} = -(A_4 + Nr)\theta_\eta(0), \tag{16}$$

and

$\mathrm{Re} = \dfrac{U_w x}{\nu_f}$ is the local Reynolds number.

Table 1: Thermophysical Properties [22, 28].

Properties	SA	MoS_2	GO
$\sigma\,(S/m)$	2.6×10^{-4}	2.09×10^{-4}	3.2×10^{-4}
$\rho(kgm^{-3})$	989	5.06×10^{3}	1800
$C_p\ (JK^{-1}Kg^{-1})$	4175	397.21	717
$\kappa\ (kgms^{-3}K^{-1})$	0.6376	904.4	5000

Thermo physical properties of hybrid nano particles obtained are defined as:

$$\left.\begin{aligned}
&\frac{\rho_{hnf}}{\rho_f}=(1-\phi_2)\left(1-\phi_1+\phi_1\left(\frac{\rho_{s_1}}{\rho_f}\right)\right)+\phi_2\left(\frac{\rho_{s_2}}{\rho_f}\right)\\
&\frac{\sigma_{hnf}}{\sigma_f}=\frac{\sigma_{s_2}+2\sigma_{bf}+2\phi_2(\sigma_{s_2}-\sigma_f)}{\sigma_{s_2}+2\sigma_{bf}-\phi_2(\sigma_{s_2}-\sigma_f)}\\
&\text{where}\\
&\frac{\sigma_{bf}}{\sigma_f}=\frac{\sigma_{s_1}+2\sigma_f+2\phi_1(\sigma_{s_1}-\sigma_f)}{\sigma_{s_1}+2\sigma_f-\phi_1(\sigma_{s_1}-\sigma_f)}\\
&\frac{\mu_{hnf}}{\mu_f}=\frac{1}{(1-\phi_1)^{2.5}(1-\phi_2)^{2.5}}\\
&\frac{D_{hnf}}{D_f}=\frac{1}{(1-\phi_1)(1-\phi_2)}\\
&\frac{(\rho C_p)_{hnf}}{(\rho C_p)_f}=(1-\phi_2)\left(1-\phi_1+\phi_1\left(\frac{(\rho C_P)_{s_1}}{(\rho C_P)_f}\right)\right)+\phi_2\left(\frac{(\rho C_P)_{s_2}}{(\rho C_P)_f}\right)\\
&\frac{\kappa_{hnf}}{\kappa_f}=\frac{\kappa_{s_2}+2\kappa_{bf}+2\phi_2(\kappa_{s_2}-\kappa_f)}{\kappa_{s_2}+2\kappa_{bf}-\phi_2(\kappa_{s_2}-\kappa_f)}\\
&\text{where}\\
&\frac{\kappa_{bf}}{\kappa_f}=\frac{\kappa_{s_1}+2\kappa_f+2\phi_1(\kappa_{s_1}-\kappa_f)}{\kappa_{s_1}+2\kappa_f-\phi_1(\kappa_{s_1}-\kappa_f)}
\end{aligned}\right\}\qquad(17)$$

3 Numerical methods with solution [2, 6, 8]

The R-K technique allows you to calculate nonlinear governing equations using partial derivatives. This approach provides more precise findings than other numerical techniques. The controlling PDEs are turned into normal differential equations by applying similarity equations. The use of additional terms reduces nonlinear equations to linear equations.

We are introducing new variables to convert upper order to a differential equation.

$$y_1=f,\ y_2=f',\ y_3=f'',\ y_4=\theta,\ y_5=\theta',\ y_6=\varphi,\ y_7=\varphi'.\qquad(18)$$

The governing equations (27) – (29) are converted to

$$y_2^1 = y_3,\ y_3^1 = -\left(\left(\frac{1}{\Lambda\left(1+\lambda^{-1}\right)}\right)\left(\frac{1}{4}y_1y_2 + \frac{1}{2}y_2^2 - M\,\mathrm{Sin}^2(\tau)\,y_2 - \left(\frac{1}{1+\lambda}\right)Da^{-1}y_2\right)\right),$$

$$y_4^1 = y_5,\ y_5^1 = -\left(\left(\frac{1}{(1+Nr)}\right)\left(A_5\,\mathrm{Pr}\,y_1y_5 + Ni\,\mathrm{Pr}\,y_4\right)\right),$$

$$y_6^1 = y_7, y_7^1 = -\left(\left(\frac{1}{A_6}\right)(Sc)\,y_1y_7 - ScCr^*\,y_6\right) \qquad (19)$$

Table 2: Comparing of $-f''(0)$ for different choices of M for

$\phi_1 = \phi_2 = Da^{-1} = \Lambda = 0,\ \tau = 90^{\bullet},\ \lambda \to \infty.$

M	Mabood and Shateyi [29]	Abood and Das [30]	Present results
0	-1.0000084	−1.000008	-1.000000
1	1.41421356	1.4142135	1.4142134
5	2.44948974	2.4494897	2.4494897
10	3.31662479	3.3166247	3.3166245
50	7.14142843	7.1414284	7.14142823

Table 3: Comparing of $-\theta'(0)$ for various choices of Pr for

$\phi_1 = \phi_2 = Nr = Ni = 0.\ \tau = 90^{\bullet},\ \lambda \to \infty.$

Pr	Mabood and Shateyi [29]	Ali [30]	Present results
0.72	0.8088	0.8058	0.809800
1	1.0000	0.9691	1.001211
3	1.9237	1.9144	1.924161
10	3.7207	3.7006	3.720400

4 Results and Discussion

The current work aims to analyze the impact of Brinkman number and variable MHD on Bi-viscous Bingham hybrid nanofluid flow across the penetrable sheet with heat transfer. Molybdenum disulphide (*MoS_2*) and Graphite oxide (*GO*) nanoparticles are dispersed in Sodium alginate (*SA*) to form a hybrid nanofluid. Using similarity conversions, the governing nonlinear PDEs for momentum, temperature, and concentration are transformed into ODEs along with the boundary condition. In the fluid region, the heat balance is kept conservative with a source/sink that relies on the temperature, and in the case of radiation, Bvp-4c, and shooting method to gain the numerical solutions. A graphical representation of several parameters is given as below and, in all graphs, solid lines denote $MoS_2 + GO / SA$ hybrid nanofluid and dashed lines denote GO / SA nanofluid.

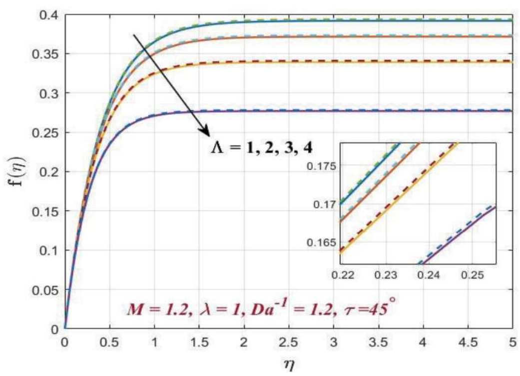

Figure 2(a): Effect of Brinkman number on transverse velocity.

Plots 2 (a) and (b) represent the transverse and axial momentum graphs for different choices of the Brinkman parameter, here solid lines denote $MoS_2 + GO / SA$ hybrid nanofluid and dashed lines denote GO / SA nanofluid. Upsurging the Brinkman number decays the velocity of the fluid movement. Physically, the Brinkman number influences fluid flow velocity by quantifying the ratio of viscous heat generation to heat conduction. As Br increases, it indicates a greater role in viscous dissipation, leading to higher flow velocities in certain conditions, particularly in non-Newtonian fluids and microchannels. This relationship is crucial for understanding flow transitions and heat transfer in various engineering applications.

Figure 3 (a) and (b) represent the transverse and axial velocity graph for different choices of the Bingham parameter. Solid lines denote the hybrid nanofluid and the dashed line denotes the nanofluid flow. Upsurging the Bingham parameter decays the momentum of the fluid flow. Physically, the momentum profile generally decays, indicating a deduction in flow velocity. This is due to the upsurged yield stress and viscosity associated with higher values of the Bingham which enhances flow resistance. Consequently, the thickness of the velocity boundary layer also decays.

Figure 4 (a) and (b) represent the transverse and axial momentum graph for various choices of the Da^{-1}. Solid lines denote the hybrid nanofluid and the dashed line denotes the nanofluid flow. Upsurging the Da^{-1} decays the velocity of the fluid movement.

Physically, this is because the upsurging in the choices of the Da^{-1} tends to decreases permeability of the porous medium suggesting increased resistance to flow due to the existence of porous fiber, resulting in transport slowdown.

Plots 5 (a) and (b) represent the transverse and axial momentum graphs for various choices of magnetic fields. Solid lines denote the hybrid nanofluid and the dashed line denotes the nanofluid flow. Upsurging the magnetic field decays the momentum of the fluid flow. Physically, this is because the Lorentz force obtained by MHD opposes the fluid flow, which can reduce the momentum of the fluid movement.

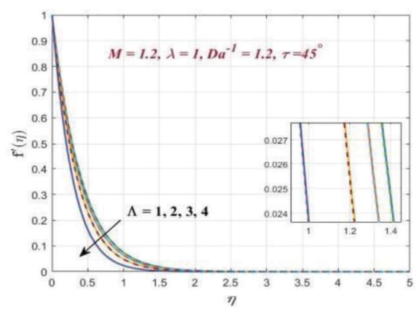

Figure 2(b): Effect of Brinkman number on transverse velocity.

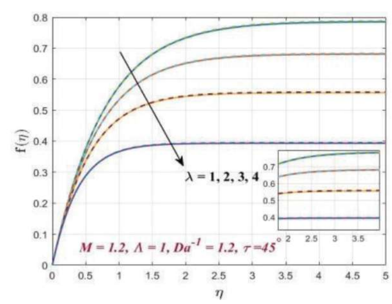

Figure 3(a): Effect of Bingham on transverse velocity.

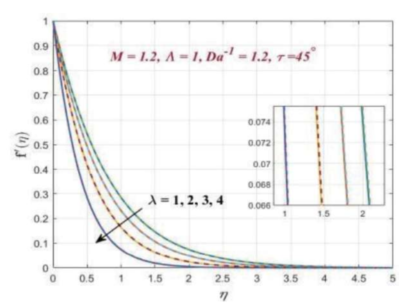

Figure 3(b): Effect of Bingham on axial velocity.

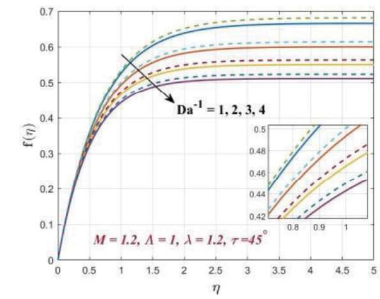

Figure 4(a): Graph of Da^{-1} on transverse velocity.

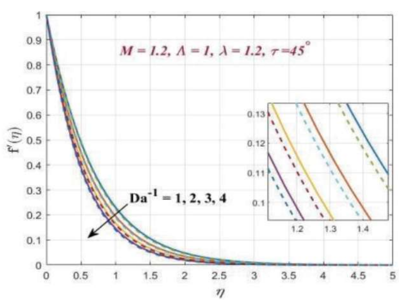

Figure 4(b): Graph of inverse Darcy number on axial velocity.

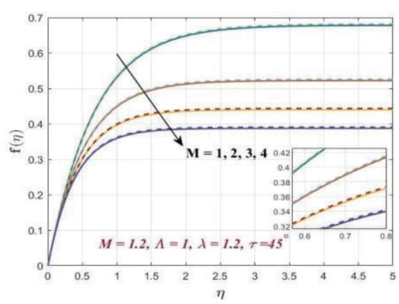

Figure 5 (a): Graph of magnetic field on transverse velocity.

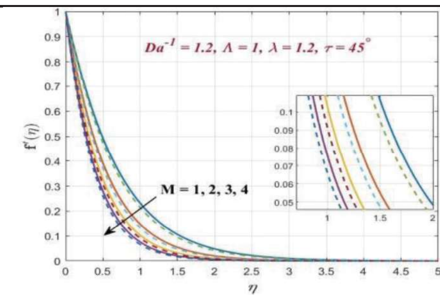

Figure 5 (b): Graph of magnetic field on axial velocity.

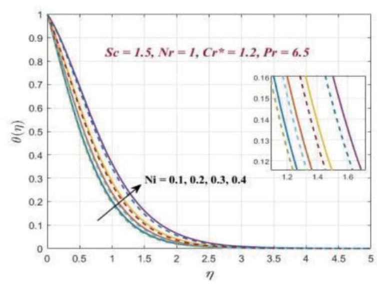

Figure 6: Influence of *Ni* on temperature.

Figure 6 portrays the temperature graph for different choices of heat source/sink. Solid lines denote the hybrid nanofluid and the dashed line denotes the nanofluid flow. Upsurging the heat source/sink increases the temperature of the liquid flow. Physically, the heat source generates more heat energy, causing the fluid temperature to upsurge.

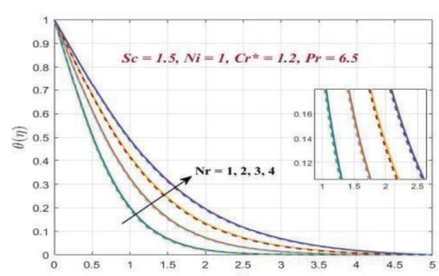

Figure 7: Impact of *Nr* on temperature.

Figure 7 portrays the temperature graph for different choices of thermal radiation. Solid lines denote the hybrid nanofluid and the dashed line denotes the nanofluid flow. Increasing the thermal radiation upsurges the temperature of the fluid flow. Physically, as the *Nr* term is upsurged, the mean absorption coefficient decays. This leads to an enlargement in the radiative heat transfer rate.

Figure 8 represents the concentration graph for various choices of Schmidt number. Solid lines denote the hybrid nanofluid and the dashed line denotes the nanofluid flow. Upsurging the *Sc* decays the concentration of the fluid flow. The physical significance of the *Sc* is to provide a measure of how efficiently a solute (such as a pollutant or a dissolved substance) is transported by diffusion compared to how efficiently it is transported by the fluid's turbulence or viscous effects.

Figure 9 represents the concentration graph for various choices of chemical reactions. Solid lines denote the hybrid nanofluid and the dashed line denotes the nanofluid flow. Increasing the Cr* parameter decreases the concentration of the fluid flow. The concentration of reactants significantly impacts the rate of a Cr*. Increasing the concentration leads to a higher number of particles in a given volume, which enhances the likelihood of collisions between reactant molecules. This increase in collision frequency results in a higher rate of successful reactions.

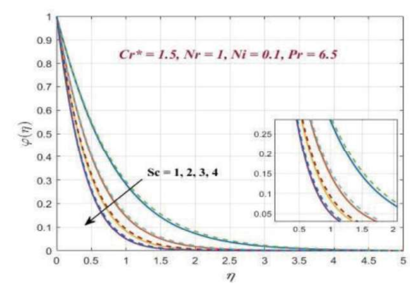

Figure 8: Impact of Schmidt number on concentration.

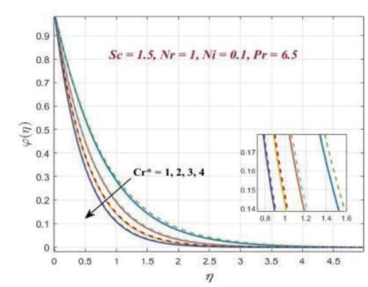

Figure 9: Graph of Cr* on concentration.

7 Conclusions

The current work aims to analyze the effect of Brinkman number and variable MHD on Bi-viscous Bingham hybrid nanofluid flow across the penetrable sheet with heat transfer. Molybdenum disulphide (*MoS_2*) and Graphite oxide (*GO*) nanoparticles are dispersed in sodium alginate (*SA*) to form a hybrid nanofluid. Using similarity conversions, the governing nonlinear PDEs for momentum, temperature, and concentration are transformed into ODEs along with the boundary condition. The results of the current work are obtained as follows:

- Upsurging the Brinkman number decays the momentum of the fluid movement.
- Upsurging the Cr* parameter decays the concentration of the fluid flow.
- Upsurging the Bingham parameter decays the velocity of the liquid flow.
- Enhancing the thermal radiation upsurges the temperature of the fluid flow.
- Increasing the magnetic field decays the velocity of flow.
- Upsurging the *Sc* decreases the concentration of the flow.
- Upsurging the Da^{-1} decays the momentum of the flow.
- Increasing the *Ni* parameter upsurges the temperature of the flow.

The limiting case of the current study are as follows:

- $\lim_{\substack{M\to 0\\ \lambda\to\infty\\ \phi_1,\phi_2\to 0\\ Nr\to 0}} \{\text{our results}\} \to \{\text{results of Wang [34]}\}.$
- $\lim_{\substack{M\to 0\\ \lambda\to\infty\\ \phi_1,\phi_2\to 0\\ Nr,Sc\to 0}} \{\text{our results}\} \to \{\text{results of Khan [36]}\}.$
- $\lim_{\substack{M\to 0\\ \lambda\to\infty\\ \phi_1,\phi_2\to 0\\ Nr,Ni\to 0}} \{\text{our results}\} \to \{\text{results of Crane [37]}\}.$

References

[1] Sachhin S. M., Mahabaleshwar U. S., Huang H. N., Sunden B., and Zeidan D., "An influence of temperature jump and Navier's slip-on hybrid nano fluid flow over a permeable stretching/shrinking sheet with heat transfer and inclined MHD", *Nanotechnology*, vol. 35(11), p. 115401, 2023, doi: 10.1088/1361-6528/ad13be.

[2] Wu Y. S., Pruess K., and Witherspoon P. A., "Flow and displacement of Bingham non-Newtonian fluids in porous media", *SPE Reservoir Engineering*, vol. 7(3), pp. 369–376, 1992, doi: 10.2118/20051-PA.

[3] Turan O., Chakraborty N., and Poole R. J., "Laminar natural convection of Bingham fluids in a square enclosure with differentially heated side walls", *Journal of Non-Newtonian Fluid Mechanics*, vol. 165(15), pp. 901–913, 2010, doi: 10.1016/j.jnnfm.2010.04.013.

[4] Vola D., Boscardin L., and Latché J. C., "Laminar unsteady flows of Bingham fluids: a numerical strategy and some benchmark results", *Journal of Computational Physics*, vol. 187(2), pp. 441–456, 2003, doi: 10.1016/S0021-9991(03)00118-9.

[5] Mahabaleshwar U. S., Anusha T., Sachhin S. M., Zeidan D., and Joo S. W., "An impact of Richardson number on the inclined MHD mixed convective flow with

heat and mass transfer", *Heat Transfer*, vol. 53(6), pp. 3104—3124, 2024, doi: 10.1002/htj.23069.

[6] Sachhin S. M., Mahabaleshwar U. S., Nayakar S. N. R., Patil H. S. R., and Souayeh B., "Darcy–Brinkman model for Boussinesq–Stokes suspension tetra dusty nanofluid flow over stretching/shrinking sheet with suction/injection", *Numerical Heat Transfer, Part A: Applications*, pp. 1—23, 2024.

[7] Siddheshwar P. G. and Mahabaleswar U. S., "Effects of radiation and heat source on MHD flow of a viscoelastic liquid and heat transfer over a stretching sheet", *International Journal of Non-Linear Mechanics*, vol. 40(6), pp. 807–820, 2005.

[8] Rahman M., Waheed H., Turkyilmazoglu M., and Siddiqui M. S., "Darcy–Brinkman porous medium for dusty fluid flow with steady boundary layer flow in the presence of slip effect", *International Journal of Modern Physics B*, vol. 38(11), p. 2450152, 2024, doi: 10.1142/S0217979224501522.

[9] Zhang L., Bhatti M. M., and Michaelides E. E., "Electro-magnetohydrodynamic flow and heat transfer of a third-grade fluid using a Darcy-Brinkman-Forchheimer model", *International Journal of Numerical Methods for Heat & Fluid Flow*, vol. 31(8), pp. 2623–2639, 2020, doi: 10.1108/HFF-09-2020-0566.

[10] Abo-Elkhair R. E., Mekheimer Kh. S., and Zaher A. Z., "Electro-magnetohydrodynamic oscillatory flow of a dielectric fluid through a porous medium with heat transfer: Brinkman model", *BioNanoscience*, vol. 8(2), pp. 596–608, 2018, doi: 10.1007/s12668-018-0515-6.

[11] Yao W., Shen Z., and Ding G., "Simulation of interstitial fluid flow in ligaments: comparison among stokes, brinkman and darcy models", *International Journal of Biological Sciences,* vol. 9(10), pp. 1050–1056, 2013, doi: 10.7150/ijbs.7242.

[12] Jena S., Mishra S. R., and Dash G. C., "Chemical reaction effect on mhd jeffery fluid flow over a stretching sheet through porous media with heat generation/absorption", *International Journal of Applied and Computational Mathematics*, vol. 3(2), pp. 1225–1238, 2017, doi: 10.1007/s40819-016-0173-8.

[13] Damseh R. A., Al-Odat M. Q., Chamkha A. J., and Shannak B. A., "Combined effect of heat generation or absorption and first-order chemical reaction on micropolar fluid flows over a uniformly stretched permeable surface", *International Journal of Thermal Sciences*, vol. 48(8), pp. 1658–1663, 2009, doi: 10.1016/j.ijthermalsci.2008.12.018.

[14] Patil P. M. and Kulkarni P. S., "Effects of chemical reaction on free convective flow of a polar fluid through a porous medium in the presence of internal heat generation", *International Journal of Thermal Sciences*, vol. 47(8), pp. 1043–1054, 2008, doi: 10.1016/j.ijthermalsci.2007.07.013.

[15] Khan A. A., Bukhari S. R., Marin M., and Ellahi R., "Effects of chemical reaction on third-grade MHD fluid flow under the influence of heat and mass transfer with variable reactive index," *Heat Transfer Research*, vol. 50(11), 2019, doi: 10.1615/HeatTransRes.2018028397.

[16] Hosseinzadeh Kh., Gholinia M., Jafari B., Ghanbarpour A., Olfian H., and Ganji D. D., "Nonlinear thermal radiation and chemical reaction effects on Maxwell fluid flow with convectively heated plate in a porous medium", *Heat Transfer—Asian Research*, vol. 48(2), pp. 744–759, 2019, doi: 10.1002/htj.21404.

[17] Alazmi B. and Vafai K., "Analysis of fluid flow and heat transfer interfacial conditions between a porous medium and a fluid layer", *International Journal of*

Heat and Mass Transfer, vol. 44(9), pp. 1735–1749, 2001, doi: 10.1016/S0017-9310(00)00217-9.

[18] Misra J. C. and Sinha A., "Effect of thermal radiation on MHD flow of blood and heat transfer in a permeable capillary in stretching motion," *Heat Mass Transfer*, vol. 49(5), pp. 617–628, 2013, doi: 10.1007/s00231-012-1107-6.

[19] Elgazery N. S., "Flow of non-Newtonian magneto-fluid with gold and alumina nanoparticles through a non-Darcian porous medium", *Journal of the Egyptian Mathematical Society*, vol. 27(1), p. 39, 2019, doi: 10.1186/s42787-019-0017-x.

[20] Coulaud O., Morel P., and Caltagirone J. P., "Numerical modelling of nonlinear effects in laminar flow through a porous medium", *Journal of Fluid Mechanics*, vol. 190, pp. 393–407, 1988, doi: 10.1017/S0022112088001375.

[21] Kaothekar S., "Thermal instability of partially ionized viscous plasma with hall effect FLR corrections flowing through porous medium", *Journal of Porous Media*, vol. 21(8), 2018, doi: 10.1615/JPorMedia.2018017559.

[22] Siddheshwar P. G., Chan A., and Mahabaleswar U. S., "Analytical study of weakly nonlinear dynamics of a Walters' liquid B around a flexible sheet undergoing super linear stretching", vol.2012(1), p. 782369, 2012.

[23] Yu D. and Wang R., "An optimal investigation of convective fluid flow suspended by carbon nanotubes and thermal radiation impact," *Mathematics*, vol. 10(9), 2022, doi: 10.3390/math10091542.

[24] Li B.W., Wang W., and Zhang J. K., "Combined effects of magnetic field and thermal radiation on fluid flow and heat transfer of mixed convection in a vertical cylindrical annulus", *Journal of Heat Transfer*, vol. 138, 2016, doi: 10.1115/1.4032609.

[25] Wissler E. H., "Viscoelastic effects in the flow of non-Newtonian fluids through a porous medium", *Industrial & Engineering Chemistry Fundamentals,* vol. 10(3), pp. 411—417, 1971, doi: https://pubs.acs.org/doi/pdf/10.1021/i160039a012.

[26] Bataller R. C., "Viscoelastic fluid flow and heat transfer over a stretching sheet under the effects of a non-uniform heat source, viscous dissipation and thermal radiation", *International Journal of Heat and Mass Transfer*, vol. 50(15), pp. 3152–3162, 2007, doi: 10.1016/j.ijheatmasstransfer.2007.01.003.

[27] Kumar M. A., Reddy Y. D., Rao V. S., and Goud B. S., "Thermal radiation impact on MHD heat transfer natural convective nano fluid flow over an impulsively started vertical plate", *Case Studies in Thermal Engineering*, vol. 24, p. 100826, 2021, doi: 10.1016/j.csite.2020.100826.

[28] Siddheshwar P. G., Chan A., and Mahabaleshwar U. S., "Suction-induced magnetohydrodynamics of a viscoelastic fluid over a stretching surface within a porous medium", *The IMA Journal of Applied Mathematics*, vol. 79(3), pp. 445–458, 2014.

[29] Mabood F. and Shateyi S., "Multiple slip effects on MHD unsteady flow heat and mass transfer impinging on permeable stretching sheet with radiation", *Modelling and Simulation in Engineering*, vol. 20(1), p. 3052790, 2019, doi: 10.1155/2019/3052790.

[30] Mabood F. and Das K., "Melting heat transfer on hydromagnetic flow of a nanofluid over a stretching sheet with radiation and second-order slip", *The European Physical Journal Plus.,* vol. 131(1), 2016, doi: https://doi.org/10.1140/epjp/i2016-16003-1.

[31] Ali M. E., "Heat transfer characteristics of a continuous stretching surface", *Wärme-und Stoffübertragung*, vol. 29(4), pp. 227-234, 1994, doi: https://doi.org/10.1007/bf01539754.

[32] Siddheshwar P. G., Mahabaleswar U. S., and Andersson H. I., "A new analytical procedure for solving the non-linear differential equation arising in the stretching sheet problem", *International Journal of Applied Mechanics and Engineering*, vol. 18(3), pp. 955–964, 2013, doi: 10.2478/ijame-2013-0059.

[33] Siddheshwar P. G., Chan A., and Mahabaleswar U. S., "An analytical study of weakly nonlinear dynamics of a Walters' liquid B around a flexible sheet undergoing super linear stretching", *ISRN Applied Mathematics*, vol. 2012, pp. 1–13, 2012, doi: 10.5402/2012/782369.

[34] Fang T. and Zhang J., "Closed-form exact solutions of MHD viscous flow over a shrinking sheet", *Communications in Nonlinear Science and Numerical Simulation*, vol. 14, pp. 2853-2857, 2009.

[35] Usafzai W. K., Aly E. H., Alshomrani A. S., and Ullah M. Z., "Multiple solutions for nanofluids flow and heat transfer in porous medium with velocity slip and temperature jump", *International Communications in Heat and Mass Transfer*, vol. 131, pp. 105831, 2022.

[36] Khan U., Zaib A., Ishak A., Roy N. C., Bakar S. A., Muhammad T., Aty A. H. A., and Yahia I. S., "Exact solutions for MHD axisymmetric hybrid nanofluid flow and heat transfer over a permeable non-linear radially shrinking/stretching surface with mutual impacts of thermal radiation", *The European Physical Journal Special Topics,* vol. 231, pp.1195–1204, 2022.

[37] Crane L. J., "Flow past a stretching plate", *Journal of Applied Mathematics and Physics*, vol. 21, p. 645, 1970.

[38] Pavlov K. B., *Magnetohydrodynamic flow of incompressible viscous fluid caused by of a surface*. M. Gidrodinamika. 4, pp. 146-147, 1974.

[39] Meng X., Artinov A., Bachmann M., and Rethmeier M., "Numerical and experimental investigation of thermo-fluid flow and element transport in electromagnetic stirring enhanced wire feed laser beam welding", *International Journal of Heat and Mass Transfer,* vol. 144, p. 118663, 2019.

[40] Li B. Q., "The fluid flow aspects of electromagnetic levitation processes", *International Journal of Engineering Science*, vol. 32(1), pp. 45–67, 1994.

Acknowledgments

Mahabaleshwar (USM) expresses profound gratitude to Senior Professor Pradeep G. Siddheshwar, F.N.A.Sc., F.I.M.A. (UK), Centre for Mathematical Needs, Department of Mathematics, CHRIST (Deemed to be University), Bengaluru – 560029, India. On the momentous occasion of his 65th birthday, we take great pride in dedicating this work to him as a token of our deep appreciation and respect. The authors also extend their sincere thanks to the reviewers for their insightful feedback, which has significantly enhanced the quality of this work.

Data Availability

Data that support the findings of this study are available from the corresponding author upon reasonable request.